Journal of Applied Engineering and Technological Science
Vol 6(2) 2025: 940-958

ANALYSIS OF PERFORMANCE AND ENERGY EFFICIENCY FOR MULTI-USER MIMO 6G NETWORK USING BEAMFORMING METHODS

Muhammad Farhan Haikal[1], Yunida Yunida[2], Nasaruddin Nasaruddin[3*]
Department of Electrical and Computer Engineering, Faculty of Engineering, Universitas Syiah Kuala, Indonesia[123]
nasaruddin@usk.ac.id

Received: 30 November 2024, Revised: 23 April 2025, Accepted: 28April 2025
**Corresponding Author*

ABSTRACT
This paper addresses the challenge of high energy consumption in sixth-generation (6G) multi-user multiple-input multiple-output (MU-MIMO) networks by analyzing how different beamforming techniques impact network performance and energy efficiency. Simulations were performed in a sub-THz communication environment using analog, digital, and hybrid beamforming across various base station antenna configurations (64, 128, and 256 elements) and user densities to evaluate performance metrics (such as received power and signal-to-interference-plus-noise ratio) alongside energy consumption. The results show that larger antenna arrays (e.g., 256 elements) provide significantly higher signal quality and received power but require more energy. In contrast, smaller arrays (e.g., 64 elements) use less power at the cost of performance. Digital beamforming with a moderate array size (128 antennas) yields the highest energy efficiency, while hybrid beamforming with the largest array results in the lowest energy efficiency. These findings imply that carefully selecting the beamforming method and antenna array size can balance performance with energy efficiency, guiding the design of more sustainable 6G networks. The novel contribution of this research is a comprehensive comparative analysis of analog, digital, and hybrid beamforming in a 6G MU-MIMO context, providing new insights for optimizing future 6G network deployments.
Keywords: *6G Network, MU-MIMO, Beamforming Techniques, Energy Efficiency, Sub-THz Communications.*

1. Introduction

Fifth-generation (5G) technologies have recently enhanced their role as foundational infrastructure for new services such as ultra-reliable low-latency communications (URLLC) and machine-type communications (Feng et al., 2021). As global demand for faster, more reliable, and efficient wireless connectivity accelerates, sixth-generation (6G) networks are anticipated to provide ultra-high data rates, low latency, and seamless integration for technologies such as the Internet of Things (IoT), autonomous systems, and immersive virtual environments. However, these advancements introduce significant challenges, particularly in terms of energy efficiency and scalable performance (Walidainy et al., 2024).

Unlike previous generations, 6G is expected to utilize both terrestrial and non-terrestrial infrastructures, including UAVs and low earth orbit (LEO) satellites, to achieve three-dimensional (3D) spatial coverage (Yu et al., 2022). Combined with operation in sub-terahertz (sub-THz) frequency bands, this architecture requires more power-intensive and directionally precise transmission technologies. Enhancing energy efficiency (EE) while maintaining high throughput is a critical design objective for 6G.

Multi-user multiple-input multiple-output (MU-MIMO) and beamforming have emerged as key technologies to meet these requirements. MU-MIMO allows a base station (BS) to serve multiple user equipment (UEs) simultaneously, improving capacity and reducing interference (Borges et al., 2021). Beamforming—whether analog (ABF), digital (DBF), or hybrid (HBF)—further enhances transmission by focusing energy toward target UEs. Each beamforming technique offers distinct trade-offs in terms of hardware complexity, energy consumption, and performance outcomes (Rihan et al., 2020; Singh & Katwe, 2023).

Recent literature explores these beamforming methods under millimeter-wave and THz communication scenarios. For instance, Ning et al. (2023) discuss ultra-massive MIMO and directional control, while Siddiqi et al. (2022) highlight the role of reconfigurable intelligent

surfaces (RIS) in next-gen networks. However, few studies provide a direct comparative evaluation of ABF, DBF, and HBF techniques in MU-MIMO systems operating at sub-THz frequencies. Moreover, the energy-performance trade-offs across different antenna configurations remain underexplored, especially in line-of-sight (LoS) scenarios involving dense user distributions.

Therefore, this study aims to:

1) Quantify the trade-offs between energy efficiency and SINR across different beamforming architectures, and
2) Identify break-even points in antenna scaling to balance energy use and system performance. MATLAB simulations are conducted using antenna arrays of 64, 128, and 256 elements in a sub-THz LoS environment to evaluate received power, SINR, and total power consumption.

The novelty of this study lies in offering a comprehensive, simulation-based comparison of beamforming strategies at the sub-THz band for 6G MU-MIMO, supported by up-to-date performance and power modeling. This work contributes valuable insights for designing energy-aware, scalable beamforming systems for future 6G deployments.

2. Literature Review

MIMO 6G

The forthcoming 6G network is expected to revolutionize wireless communications by accommodating a vast number of devices, providing ultra-high data speeds, ensuring ultra-low latency, and facilitating smoother connectivity (Meena et al., 2022). However, one of the primary challenges in designing the 6G network is enhancing energy efficiency. The growing demand for wireless services, combined with environmental concerns over high energy consumption in communications networks, drives the research focused on improving energy efficiency.

MIMO technology is a fundamental component of next-generation wireless communication systems, including 6G, as shown in Figure 1. In an MU-MIMO system, a base station (BS) equipped with multiple antennas can communicate simultaneously with several users, thereby enhancing capacity and spectral efficiency. The incorporation of a large number of antennas has become a hallmark of the 5G network, leading to the development of massive MIMO (Muharar et al., 2024). By greatly increasing the number of elements in the antenna array compared to traditional MIMO systems, massive MIMO can significantly enhance the spectral and energy efficiency of wireless communications. The presence of many antennas enables the creation of highly directional beams, allowing the base station to serve multiple users simultaneously using the same time and frequency resources. This highly focused beam also allows the base station to concentrate energy specifically on the intended user. In 6G networks, which are expected to support a very large number of users, MU-MIMO is crucial for achieving higher capacity, more reliable communications, and low latency. MU-MIMO leverages spatial diversity to enhance system capacity without increasing power consumption. Therefore, the energy needed to support communication with many users can be minimized, especially when combined with optimal beamforming techniques.

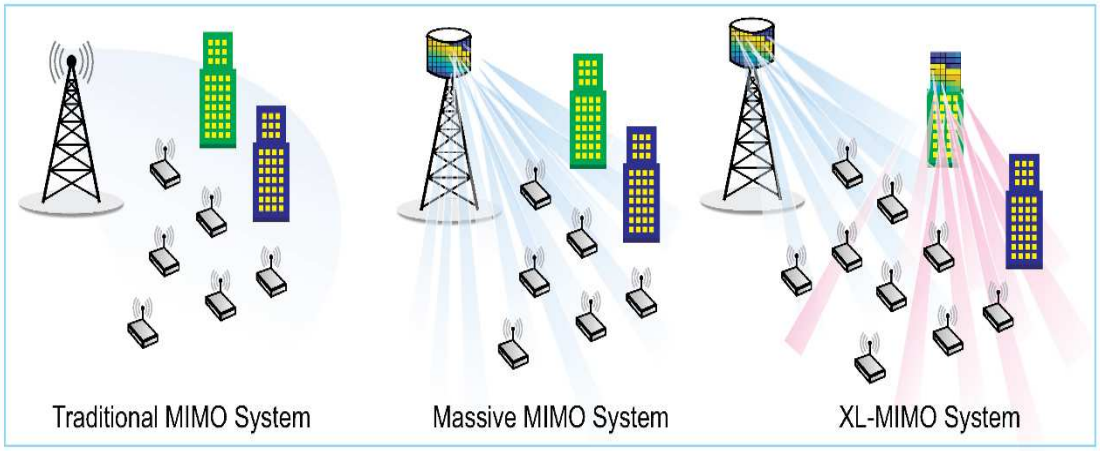

Fig. 1. Traditional MIMO, mMIMO, and XL-MIMO systems (Dala Pegorara Souto et al., 2023)

Beamforming Methods

The upcoming 6G network is poised to revolutionize wireless communication by providing ultra-reliable, low-latency, and high-speed connectivity across terrestrial and non-terrestrial platforms (Meena et al., 2022). Central to this capability is the adoption of MU-MIMO systems, which enhance spectral efficiency by allowing base stations to serve multiple user equipment (UEs) simultaneously. MU-MIMO's effectiveness depends heavily on its antenna configuration and signal-processing techniques, particularly beamforming.

Beamforming is a critical technique for shaping the radiation pattern of antennas to improve directionality and signal quality. It can be implemented through analog, digital, or hybrid techniques, as illustrated in Figure 2, each offering distinct trade-offs regarding complexity, cost, and performance (Rihan et al., 2020). Analog beamforming (ABF) is cost-efficient but lacks flexibility; digital beamforming (DBF) allows precise control at the cost of higher power consumption; and hybrid beamforming (HBF) aims to balance these trade-offs. (Ning et al., 2023). For example, HBF emphasized its promise for mmWave due to reduced hardware cost. However, our results suggest that at sub-THz frequencies, DBF provides superior energy efficiency, particularly with 128-antenna configurations, challenging the generalization of previous findings to higher frequency bands.

Analog beamforming primarily aims to use low-cost phase shifters to control the phase of the transmitted signal for each element in an antenna array. This system comprises multiple antennas, an RF chain connected to a phase shifter, baseband processing, and an analog-to-digital converter (ADC). In contrast, digital beamforming utilizes digital signal transmission for each element of the antenna array to manipulate the shape of the beam in the digital domain. Digital beamforming architectures require dedicated ADCs and RF chains for each antenna component, and the signals are processed separately in the baseband domain. DBF can be categorized into two types: fixed and adaptive. Fixed DBF maintains its preset antenna configuration and phase, which cannot be altered during communication. On the other hand, adaptive DBF features antennas that can be modified to meet specific requirements, such as enhancing the signal-to-noise ratio (SNR) and directivity at particular locations or adjusting the beam shape to navigate around obstacles. The hybrid beamforming (HB) architecture operates in both the baseband and analog domains. It has been shown to achieve digital beamforming performance in certain scenarios while significantly reducing hardware costs and power consumption. Three main types of HB architectures have been widely reported: fully connected, partially connected (also known as array-of-subarray, or AoSA), and dynamically connected architectures.

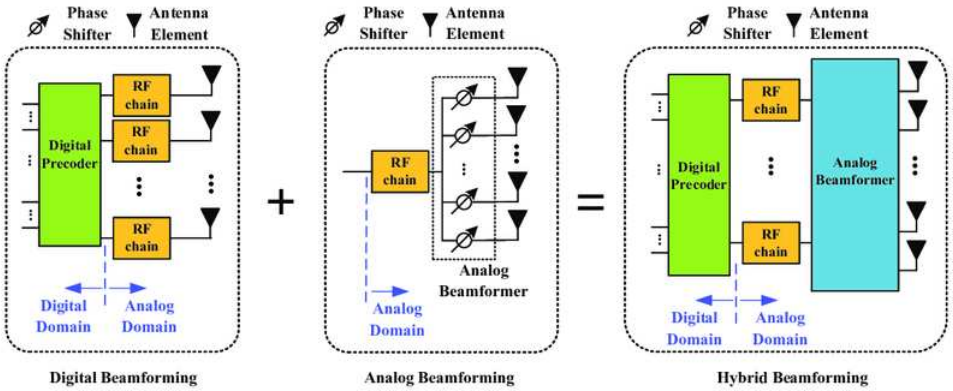

Fig. 2. Beamforming methods for 6G (Ning et al., 2023)

Energy Efficiency

6G MU-MIMO systems play a crucial role in enhancing network capacity and improving spectrum usage efficiency (Damsgaard et al., 2023). This new technology is expected to significantly outperform 5G MU-MIMO systems by utilizing higher frequency spectrums, such as mmWave and sub-THz, as well as implementing artificial intelligence (AI) and machine learning (ML) techniques for better coverage optimization and signal quality. Enhancing MU-MIMO performance in 6G is essential to meet the growing demands for higher data capacities and broader connectivity. Systems that combine high-frequency technologies with AI and machine learning hold the potential to address various challenges, such as interference, spectrum management, and energy efficiency optimization. With these advancements, MU-MIMO could serve as the backbone of a faster, more reliable, and efficient 6G network.

Energy efficiency in a 6G MU-MIMO system is influenced by several factors as follows:

a) Base stations with multiple antennas consume more power, particularly when using complex beamforming methods. Thus, optimizing the power consumption of the beamforming algorithm and antenna configuration is crucial for enhancing energy efficiency.
b) In high-density user environments, like urban areas, managing power consumption is more challenging. Beamforming helps reduce user interference, enabling more efficient power usage in these situations.
c) Beamforming enhances spectral efficiency by directing power specifically to users who require a strong signal. This approach allows for a greater amount of data to be transmitted per unit of power. As a result, energy efficiency improves, as more users can be served simultaneously without a proportional increase in power consumption.
d) Channel Conditions and Propagation: Physical channel conditions, including signal loss, multipath propagation, and interference, influence the performance of beamforming techniques. In poor channel conditions, advanced beamforming techniques and increased power levels may be required to ensure the desired signal quality.

Regarding the factors mentioned above, the parameters of the 6G sub-terahertz telecommunications antenna used in this research are presented in Table 1.

Table 1 - 6G sub-terahertz telecommunication parameters

No	Parameter	Value
1.	Working frequency (f)	142 GHz (Rappaport et al., 2019)
2.	Bandwidth (B)	7 GHz
3.	Gain antenna base station (G_{Tx})	27 dBi
4.	Base station transmitter power (P)	30 dBm (Saeed et al., 2023)

The path loss immersion factor refers to the reduction in signal strength experienced during transmission in free space, primarily due to the power absorbed by the atmosphere. This phenomenon is known as free space loss (FSL). The FSL between two communication antennas that are separated by a distance "d" in kilometers (km) and operating at a frequency "d" in gigahertz (GHz) can be calculated as follows (Maccartney et al., 2015).

$$L_{fsl}[dB] = 92.4 + 20log f_{[GHz]} + 20\log d_{[km]} \quad (1)$$

The power loss along each communication path, commonly referred to as Path Loss (PL), is attributed to non-line-of-sight (NLOS) conditions between two antennas that are separated by a distance "d" measured in kilometers (km). These antennas operate at a frequency "f" in gigahertz (GHz). The variable $X\sigma$ represents a Gaussian random variable with a mean of zero and a standard deviation (antenna deviation), σ, expressed in decibels (dB). The standard deviation can be derived from the reference (Maccartney et al., 2015).

$$PL(d) = PL(d_0) + 10nlog_{10}\left(\frac{d}{(d_0)}\right) + X_\sigma \quad (2)$$

where the $PL(d_0)$ value is obtained from close-in free space damping using a reference distance $d_0 = 1$ (Maccartney et al., 2015).

$$PL(d_0) = 10log_{10}\left(\frac{4\pi d_0}{\lambda}\right)^2 \quad (3)$$

The λ value is determined by the wave antenna being used. As the λ value increases, the frequency decreases. Similarly, a larger λ results in reduced path damping. The specific rain frequency increases exponentially in both light and heavy rain at a given rain rate (R in mm/hour). To better understand the environmental constraints of operating in the sub-THz band, Figure 3 illustrates the frequency-dependent rain attenuation based on the ITU-R model with a rain rate of 25 mm/h. The attenuation is computed using the empirical equation:

$$\gamma_{Rain}\left[\frac{dB}{Km}\right] = kR^{\alpha} \quad (4)$$

where k is 0.1964 and the attenuation α is 0.9277 at a working frequency from the range 1 GHz $\leq f \leq$ 1000 GHz (Hemadeh et al., 2018; (Hemadeh et al., 2018; International Telecommunication Union Radiocommunication Sector, 2005). As seen in Figure 3, attenuation increases significantly with frequency, particularly beyond 120 GHz. This behavior emphasizes the practical limitations of using higher sub-THz frequencies for long-range communication, especially under adverse weather conditions. The inclusion of this attenuation curve provides context for selecting 142 GHz as the working frequency in this study, balancing between bandwidth availability and manageable propagation loss. It also justifies the need for advanced beamforming techniques, such as MU-MIMO, to maintain energy-efficient transmission in these challenging frequency environments.

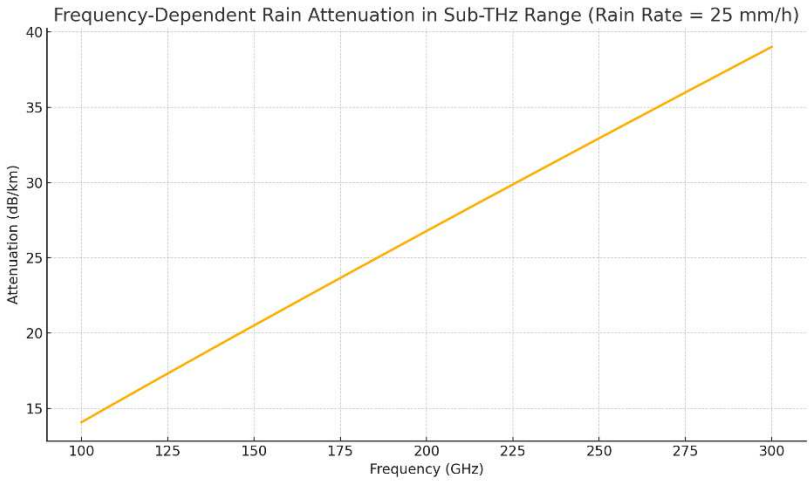

Fig. 3 Rain Attenuation As A Function Of Frequency In The sub-terahertz (sub-THz) band, calculated using the ITU-R model for a rain rate of 25 mm/h.

The received power is the isotropic power level detected by the receiving station. The antenna's receiving power level from the station can be expressed as (Rinanda, 2019):

$$P_{rx_k} = P - L_{total}[dB] \quad (5)$$

where P_{rx_k} is received power at k th UE (dBm), P is transmitted power BS (dBm), and L_{total} is the total of signal attenuation (dBm).

The difference between the received signal power and the combined power of interference and noise is known as the Signal Interference Plus Noise Ratio (SINR). Over 24 hours, interference plays a significant role in the design and performance analysis of wireless networks. This occurs when a desired antenna signal is mixed with an unwanted signal originating from another source, sharing the same frequency, spatial location, or time slot. SINR with two intended transmitters and receivers, each represented by *i*. The transmitters have the potential to interfere with the communication between the transmitter and the intended receiver, which can be expressed as (Banday et al., 2020):

$$SINR_k = \frac{P_{Rx_k}}{\sum_{i \neq k}^{K} P_{Rx_i} + N_k} \quad (6)$$

where $SINR_k$ is the SINR at k th UE (dB), P_{Rx_k} is received power at k th UE (dBm), $P_{R_{x_i}}$ is interference power at 1st UE (dBm), and N_k is noise power at k th UE (dBm). Factors such as transmit power, interference management, antenna pattern, and the beamforming antenna used affect signal power and interferer k.

The trade-offs between signal quality and power consumption in 6G beamforming systems are best understood through the lens of the Shannon-Hartley theorem, which relates to data rate. Data rate is the speed at which information is sent or received, measured in bits per second. This data rate is calculated to determine how quickly information travels from the transmitter to the receiver (Walrand & Varaiya, 2014).

$$R_k = \frac{B}{2}\log_2\left(1 + SINR_k\right) \quad (7)$$

where R_k is the data rate at k th UE (bit/s), B is bandwidth (Hz), and $SINR_k$ is signal-to-interference plus noise ratio (dB).

In urban areas, supplying adequate power to the antenna at the base station is crucial. As the number of internet users increases, the power consumption of cellular communication antennas at the base station also rises. The following devices tend to consume a significant amount of power (Ahmed et al., 2022):

- Digital signal processing (DSP) is used for digitizing analog signals and processing them.
- The amplifier is responsible for converting DC input power into a significant RF signal.
- Air conditioning (AC) helps maintain suitable temperatures, ensuring that base station equipment operates smoothly.
- The backhaul link connects the backhaul network to the base station, using either a microwave or fiber connection.
- A transceiver is a device used for both transmitting and receiving signals at the base station.
- Rectifier is AC to DC converter.

To determine the amount of force applied to the BS, the appropriate equation can be utilized (Matalatala et al., 2017).

$$P_{ABF} = N_{ant} \cdot \left(\eta \cdot P_{amp}\right) + P_{trans} + P_{rect} + P_{cool} + P_{bhl} \quad (8)$$

$$P_{DBF} = N_{ant} \cdot \left(P_{trans} + P_{dsp} + \eta \cdot P_{amp}\right) + P_{rect} + P_{cool} + P_{bhl} \quad (9)$$

$$P_{HBF} = N_{ant} \cdot \left(\eta \cdot P_{amp}\right) + M_{trans} \cdot P_{trans} + P_{dsp} + P_{rect} + P_{cool} + P_{bhl} \quad (10)$$

where N_{ant} is the element number of BS, P_{trans} is transceiver RF power (W), P_{dsp} is the consumed power unit of DSP (W), η is the efficiency of the amplifier, P_{amp} is the power consumption of the antenna amplifier (W), P_{rect} is rectifier power (W), P_{cool} is the AC power consumption (W), P_{bhl} is link backhaul power (W), P_{ABF} is the power consumption for

Analog *Beamforming* (W), P_{DBF} is the power consumption for Digital *Beamforming* (W), P_{HBF} is the power consumption for hybrid *beamforming* (W), and M_{trans} is the number of RF antenna *transceiver*s.

Table 2 - Power consumption at base station 6G (Matalatala et al., 2017)

No.	Parameter	Description	value
1.	P_{trans}	Transceiver power per antenna branch	1.5 W
2.	η	Power amplifier efficiency	50%
3.	P_{bhl}	Backhaul power	10 W
4.	P_{cool}	Antenna cooler power	200 W
5.	P_{rect}	Rectifier power	50 W
6.	P_{dsp}	The signal processing power of each antenna branch	1 W

Mobile communications networks contribute a small portion to the overall carbon footprint of Information and Communication Technologies (ICTs), accounting for approximately 0.2% of global emissions as part of the antenna sector (Al-Yasir et al., 2022). The following equations were used to calculate energy efficiency (EE).

$$EE_{ABF} = \frac{R_{sum}}{P_{ABF}} \quad (11)$$

$$EE_{DBF} = \frac{R_{sum}}{P_{DBF}} \quad (12)$$

$$EE_{HBF} = \frac{R_{sum}}{P_{HBF}} \quad (13)$$

where R_{sum} is the total data rate (bit/s), P_{ABF} is the total consumed power for analog beamforming (W), P_{DBF} is the total consumed power for digital beamforming (W), and P_{HBF} is the total consumed power for hybrid beamforming (W).

While extensive work has been done on beamforming and MIMO in mmWave bands (Nasaruddin et al., 2023), comparative studies across ABF, DBF, and HBF in the sub-THz spectrum remain scarce. Most existing studies either focus on a single beamforming approach or do not comprehensively analyze the energy-performance trade-offs for varying antenna scales. Furthermore, the interaction between EE and SINR across beamforming methods under dense UE scenarios remains underexplored. This research fills that gap by simulating and contrasting three beamforming types under realistic sub-THz propagation conditions, offering a more holistic view.

3. Research Methods

System Model for MIMO 6G

The 6G MIMO system model depicted in Figure 4 consists of one base station (BS) and eight user equipment (UE) devices, positioned 25 m apart from each other. The antenna configuration utilizes the Line of Sight (LoS) technique. The base station is equipped with antennas mounted at a height of 15 m, while the UEs have antennas at a height of 1.5 m. The distance from the base station to the farthest point in the cell is 200 m. This system employs multiple antennas on both the base station and the UEs to facilitate simultaneous signal transmission and reception. These features help to reduce interference and enhance signal quality. Additionally, digital signal processing technology is implemented to manage and optimize both transmitted and received signals, incorporating techniques such as beamforming and various coding methods. The backhaul network is a crucial component that links the base station with the core network, ensuring efficient data transfer.

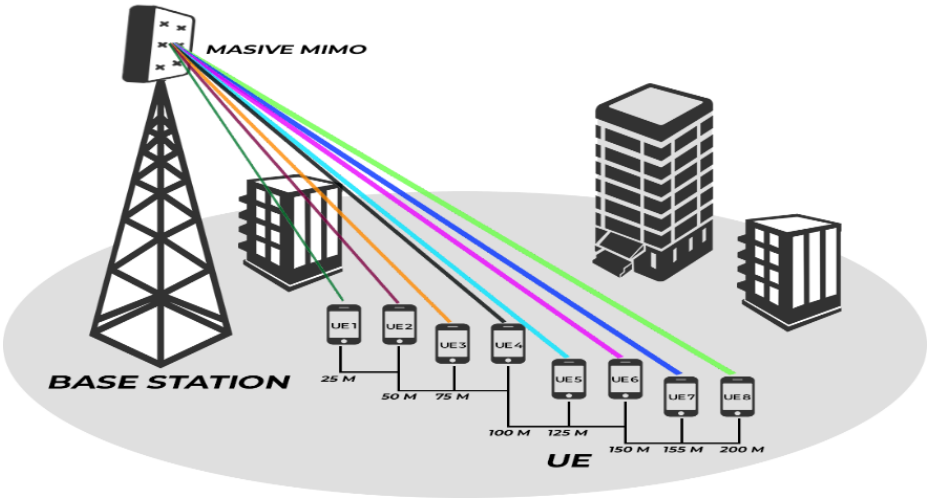

Fig. 4. System model for MU MIMO 6G

Table 3 - Parameters for the system model

No.	Parameter	Value
1.	Frequency type	Sub-Terra Hertz
2.	Carrier frequency	142 GHz (Rappaport et al., 2019)
3.	Bandwidth	7 GHz
4.	Propagation method	LOS
5.	Base station power transmission	30 dBm (Saeed et al., 2023)
6.	Number of antennas at Base Station	64, 128, 256 (Jing et al., 2016)
7.	Number of antennas at UE	1 (Jing et al., 2016)
8.	Noise Figure	10 dB (Saeed et al., 2023)
9.	Number of Base Stations	1
10.	Number of UEs	8
11.	Cell radius	200 m

Simulation of Performance Parameters and Energy Efficiency

This study employs a simulation-based approach to evaluate the performance and energy efficiency of various beamforming techniques in a 6G multi-user MIMO system. Simulations were conducted using MATLAB 2022, utilizing the Phased Array System Toolbox and Antenna Toolbox to model antenna behavior, signal propagation, and beamforming operations in a sub-terahertz (sub-THz) environment. The system model comprises a single base station (BS) equipped with a variable number of antennas (64, 128, and 256 elements) communicating with eight UE nodes, each spaced 25 meters apart. The communication channel is assumed to be LOS, which is typical in high-frequency sub-THz scenarios due to reduced multipath effects and stronger directional propagation. In this study, we selected the LoS model to focus on the effects of beamforming performance, aligning with previous 6G sub-THz research that highlights strong direct-path dominance, instead of using Rician fading models commonly applied in mmWave systems.

To further strengthen realism, we acknowledge the 3GPP TR 38.901 channel model, which is widely used in 5G evaluations. However, its parameters are tailored for frequencies up to 100 GHz. Since this study operates at 142 GHz, a simplified LoS propagation model was chosen for clarity and computational efficiency, with atmospheric attenuation (including rain and gas) added based on ITU-R and Rappaport et al. models. Atmospheric attenuation is calculated using Equation (4). Rain and gas attenuation are measured with the MATLAB toolbox, which can be accessed through MATLAB algorithms. The results of the attenuation measurements from the base station to each UE will be combined with the atmospheric attenuation. The sum of these values will give the total attenuation. The received power is then determined by subtracting the transmit power from the base station from the total attenuation. This calculation will provide the value of the received power.

Three types of beamforming architectures were implemented:

1) Analog Beamforming (ABF): Utilizes a single RF chain with phase shifters applied to control signal directionality.
2) Digital Beamforming (DBF): Applies digital signal processing at each antenna element, offering full flexibility but with higher power demands.
3) Hybrid Beamforming (HBF): Combines analog and digital layers to reduce complexity while approximating DBF performance.

Each beamforming method was tested under the same environmental and distance conditions, with antenna elements arranged in uniform rectangular arrays. Signal attenuation was calculated using standard free-space and atmospheric loss models. Received power was derived by subtracting the total path loss from the transmit power. Signal-to-Interference-plus-Noise Ratio (SINR) was computed based on received power, modeled interference, and noise values. The data rate was calculated using the Shannon-Hartley theorem. Energy efficiency (EE) was defined as the ratio of total throughput to total power consumption (Mb/s/W), where power components included amplifier usage, baseband processing, and cooling systems. To ensure regulatory compliance, all simulation parameters were verified against FCC electromagnetic field (EMF) exposure limits, ensuring that total transmit power and beamforming gains remained within safe exposure thresholds.

4. Results and Discussions

Implemented Simulation Model

This research begins by positioning the microsites according to the specific research location. The beam direction for the micro base transceiver station (BTS) is set at an angle of 150°. The beams are directed towards eight UE devices located at distances of 25 m, 50 m, 75 m, 100 m, 125 m, 150 m, 175 m, and 200 m, respectively. These beams utilize beamforming techniques with antennas configured in a Uniform Rectangular Array (URA) consisting of 64, 128, and 256 antennas. The results of the MATLAB simulations can be seen in Figures 5 and 6. The placement of these micro base stations is crucial as they are designed to enhance network coverage in smaller or more densely populated areas. Proper positioning of the micro-sites significantly affects the efficiency of spectrum usage, power distribution within the network, and the quality of the signal received by users. In this paper, the micro site's design incorporates a beam angle of 150°, indicating that the coverage area served by the micro BTS is 150 degrees wide. This angle allows the micro BTS to focus on a specific area with a high density of users. The selective beam area optimizes power distribution and minimizes interference from users outside the designated coverage area.

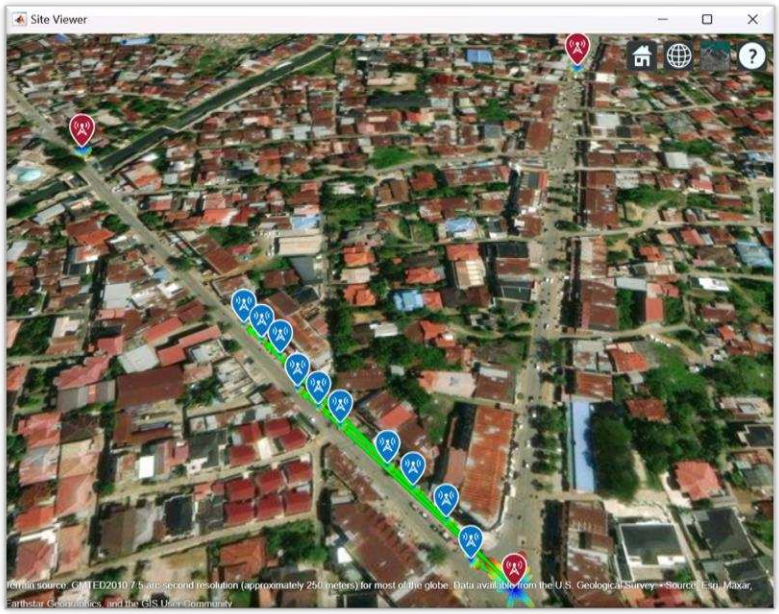

Fig. 5. Network Simulation Model from Satellite View

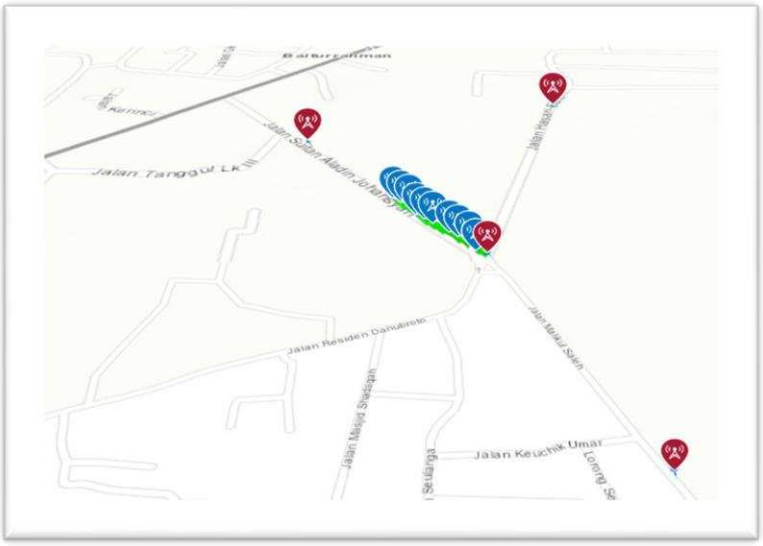

Fig. 6. Topography of the simulation model

Figure 6 illustrates that the red tower symbol represents the BTS as the transmitter, while the blue symbol represents the UE as the receiver. The BTS located in the center is the desired signal for the UE, and the other symbols represent sources of interference for the UE. The distance between each BTS is 400 meters, while the distance between UEs is 20 meters. The green line in the figure indicates the line of sight (LOS) conditions between the BTS and the UE.

Total Attenuation

The simulation results for total attenuation, or path loss, during signal propagation, were obtained after configuring the BTS and the UE. These results are illustrated in Figure 7. The figure demonstrates that the lowest signal power loss occurs at 64 antennas positioned at 40 meters, with the attenuation increasing as the distance from the UE extends from 100 meters to 200 meters. In comparison, the total attenuation for 128 and 256 antennas exceeds that of 64 antennas; however, after 100 meters, they exhibit the smallest total attenuation. This variation is attributed to the Doppler effect, which refers to the change in the frequency of a wave received by the UE due to the relative movement between the base station and the UE. The average power attenuation for configurations with 64, 128, and 256 antennas is measured at 116.02 dB, 110.012 dB, and 109.583 dB, respectively.

At greater distances, specifically between 100 m and 200 m, communication channels are more significantly influenced by propagation effects. These effects include signal attenuation due to distance, physical obstacles, and interference. In this context, the benefits of having a larger number of antennas become more apparent. With more antennas, BTS can direct signal power more precisely toward users located farther away. This targeting helps to reduce interference both from other users and the environment, ultimately enhancing the quality of the signal received by UEs, even over greater distances.

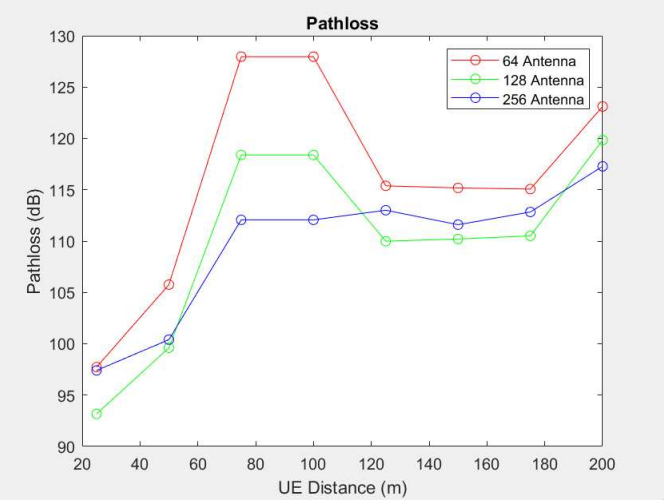

Fig. 7. Total Attenuation With The Different Number Of Antennas

Moreover, advanced beamforming techniques that utilize a greater number of antennas can effectively address multi-path fading, which is the phenomenon caused by reflected waves that diminish signal strength. This effect becomes more pronounced as the distance increases. Consequently, although the total signal attenuation with 128 and 256 antennas is higher at short distances, their enhanced ability to direct signals more efficiently over longer distances results in reduced total attenuation after 100 meters.

The configurations with 64, 128, and 256 antennas demonstrate that a greater number of antennas enhances the system's ability to direct signals to specific users. However, at certain distances, such as 40 meters, the configuration with 64 antennas exhibits less attenuation. In contrast, at longer distances (between 100 and 200 meters), systems with 128 and 256 antennas show less attenuation compared to those with 64 antennas.

At very short distances, a system with 64 antennas effectively directs signals to nearby user equipment (UEs), resulting in low attenuation. However, as the distance increases, this limited number of antenna elements diminishes the system's ability to counteract obstructions and interference from other users, leading to increased attenuation. While systems with 128 and 256 antennas may experience higher attenuation at closer distances (for example, at 40 meters), they are more effective in reducing attenuation at longer distances (100 to 200 meters). The presence of more antenna elements optimizes the ability to perform beamforming with greater precision, which reduces interference and mitigates the effects of poor channel conditions at longer distances, particularly when the Doppler effect becomes more pronounced.

The simulation results reveal that as the number of base station antennas increases from 64 to 256, signal attenuation decreases significantly in mid-to-long-range communication (100–200 m), primarily due to improved directional gain and reduced beam divergence. The 256-antenna configuration demonstrates the lowest average attenuation at 109.58 dB, compared to 116.02 dB for 64 antennas. This confirms the advantage of large-scale antenna arrays in maintaining signal strength over longer distances—an essential requirement for 6G networks, which aim to deliver high-capacity and low-latency services over broad spatial coverage.

Received Power and SINR

The simulation results for received power were obtained after calculating the path loss. The received power results can be seen in Figure 8. According to Figure 8, at a distance of 100 meters, the highest received power was observed with 64 antennas. However, after reaching 60 meters, the maximum received power was recorded with 128 antennas. Between the distances of 180 to 200 meters, the 256 antennas demonstrated the highest receiving power. The variation in received power at different distances is attributed to the focus area of the antenna beam and the beamforming center of the signal, which differ for each configuration. At shorter distances, the 64 antennas perform better due to their less focused beams compared to the 128 and 256 antennas. Conversely, at longer distances, the 128 and 256 antennas achieve better performance because their beams are more focused. The received power measured with 64 antennas is lower

compared to the 128 and 256 antennas because of higher path loss, resulting in greater signal attenuation. Consequently, the average received power for the configurations is as follows: 64 antennas yield -68.0203 dBm, 128 antennas provide -62.0124 dBm, and 256 antennas achieve -61.5833 dBm.

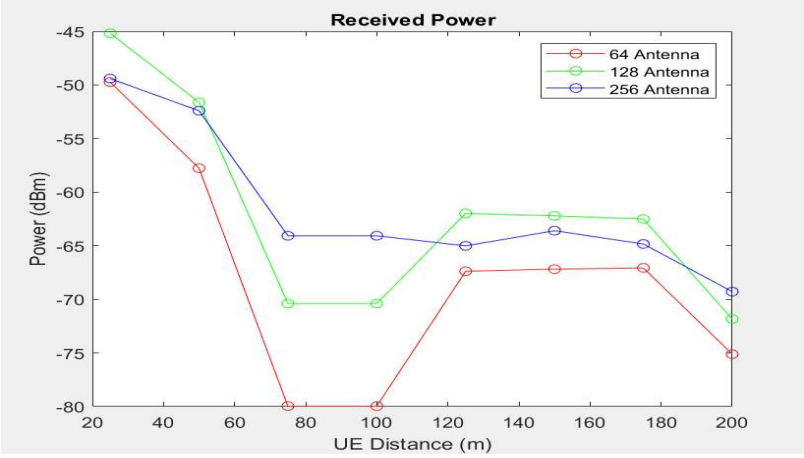

Fig. 8. Received power with different number of antennas

The SINR simulation results are obtained by comparing the received signal power to the combined values of interference and noise power. The average interference for each UE is displayed in Figure 9. Specifically, the average interference values for antennas with 64, 128, and 256 elements are -134.124 dBm, -127.72 dBm, and -127.307 dBm, respectively.

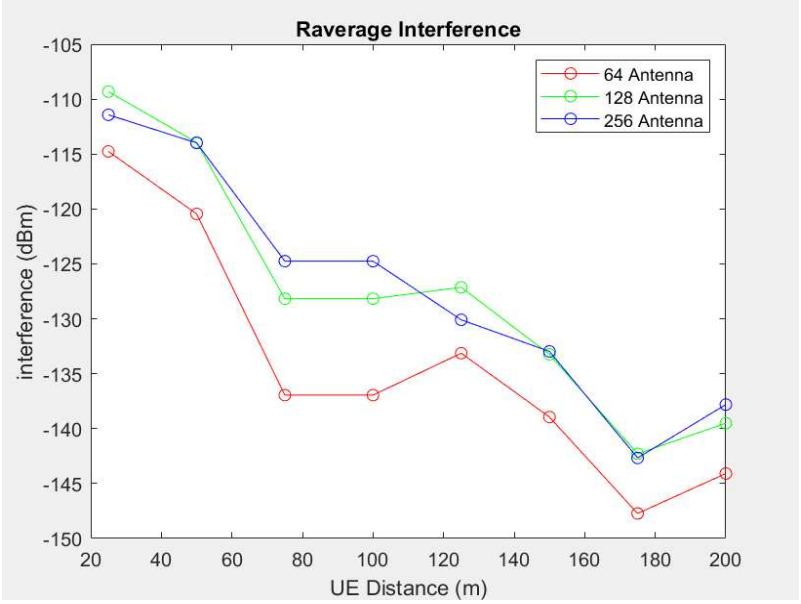

Fig. 9. Average interference with the different number of antennas

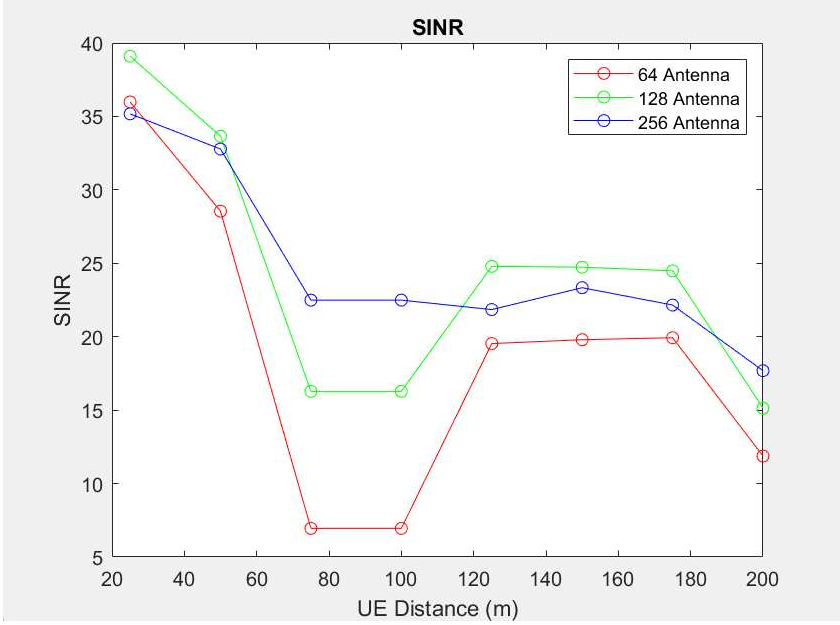

Fig. 10. SINR Simulation Results

Based on the interference values shown in Figure 8, the SINR is illustrated in Figure 10. The results from the SINR simulation are derived by comparing the received power of each User Equipment (UE) with the combined noise power and interference power. The average SINR values for configurations with 64, 128, and 256 antennas are 18.6953, 24.3074, and 24.7454 dBm, respectively. The figure indicates that the highest SINR value occurs with 64 antennas at a distance of 40 meters. As the distance increases between 80 and 180 meters, the highest SINR shifts to the configuration with 128 antennas. At a distance of 200 meters, the configuration with 256 antennas provides the highest SINR value. Fluctuations in the SINR result from variations in the received power obtained by the UE, and they are also influenced by interference levels affecting the UE.

In terms of received power and SINR, the 256-antenna configuration achieves the best performance, with average received power at -61.58 dBm and SINR at 24.75 dB. These values exceed those reported in Damsgaard et al. (2023), where mmWave SINR values averaged 20.5 dB. The 4.2 dB improvement can be attributed to increased beam directivity and minimized interference, especially in LoS propagation. Notably, while increasing antenna count improves performance, it also leads to higher energy consumption.

Data Rate

The results of the data rate simulation were obtained using Equation (7) and are illustrated in Figure 11. This figure displays the data rate simulation results for each antenna configuration and each UE. The average data rates for the configurations with 64, 128, and 256 antennas are 205.54, 229.51, and 232.74 Mbps, respectively. The data rate obtained in the simulation shows a pattern that closely resembles the SINR pattern. This correlation occurs because the data rate is directly proportional to SINR; thus, higher SINR values lead to higher data rates. Additionally, the fluctuating data rate values are influenced by the SINR values experienced by each UE.

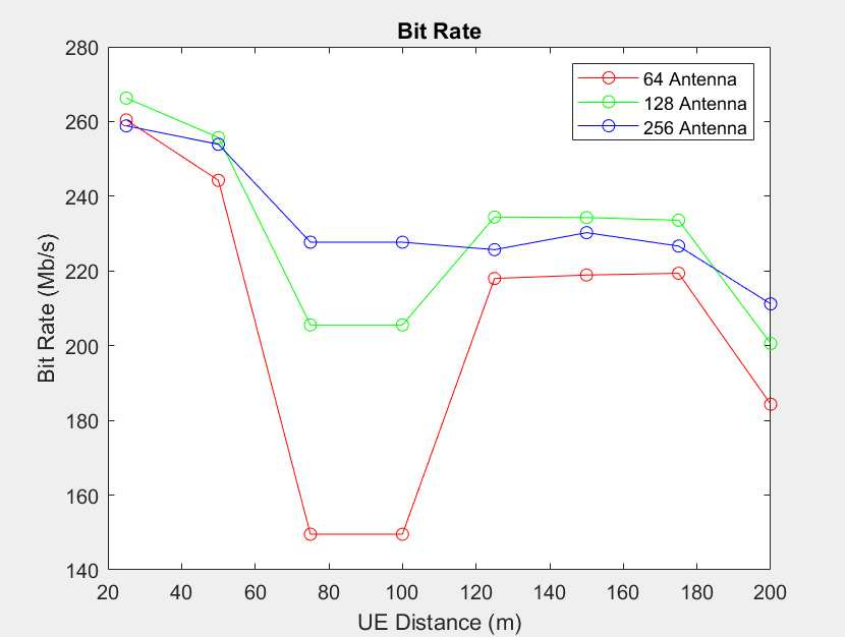

Fig. 11. Bit Rate Simulation Results

Power Consumption

Power consumption is calculated using equations (8) to (10) with the parameter values provided in Table 2. The results of these power consumption calculations are presented in Tables 4 and 5.

Table 4 - Power consumption for beamforming methods in Watt

Beamforming	64 Antennas	128 Antennas	256 Antennas
PDBF	327 W	335 W	343 W
PABF	687 W	888 W	1089 W
PHBF	864 W	1065 W	1266 W

Table 5 - Power consumption for beamforming methods in dBm

Beamforming	64 Antennas	128 Antennas	256 Antennas
PDBF	55,54 dBm	55,25 dBm	55,35 dBm
PABF	58,37 dBm	59,48 dBm	60,37 dBm
PHBF	59,36 dBm	60,27 dBm	61,02 dBm

Table 4 presents the power consumption values for configurations using 64, 128, and 256 antennas with PDBF, PABF, and PHBF settings. The results indicate that PDBF has the lowest power consumption compared to PABF and PHBF. In contrast, PHBF consumes the most power across all antenna configurations. This breakdown offers a clear comparison of power consumption among the different antenna configurations. In addition, as the number of antennas increases, so does the power consumption.

Table 5 provides the power consumption values in dBm for different antenna systems. According to the table, the 256-element DBF antenna has a power consumption of 55.35 dBm, while the ABF antenna consumes 60.37 dBm, and the HBF antenna consumes 61.02 dBm. For the 128-element DBF antenna, the power consumption is 55.25 dBm, with the ABF antenna using 59.48 dBm and the HBF antenna consuming 60.27 dBm. The 64-element DBF antennas have a power consumption of 55.54 dBm, the ABF antennas consume 58.37 dBm, and the HBF antennas use 59.36 dBm. The PABF system exhibits higher power consumption due to its use of more antennas and UE devices, while the PDBF system operates with fewer devices. However, the PHBF system has the highest overall power consumption since it incorporates all the devices from both the PDBF and PABF systems.

Energy Efficiency

The energy efficiency simulation results are categorized into three types: EE DBF, EE ABF, and EE HBF. These results display the energy efficiency based on the number of antennas and user equipment (UEs). The energy efficiency values are derived from equations (11) to (13).

For a visual representation, the simulation results for EE ABF, EE DBF, and EE HBF can be found in Figures 11 to 13, respectively.

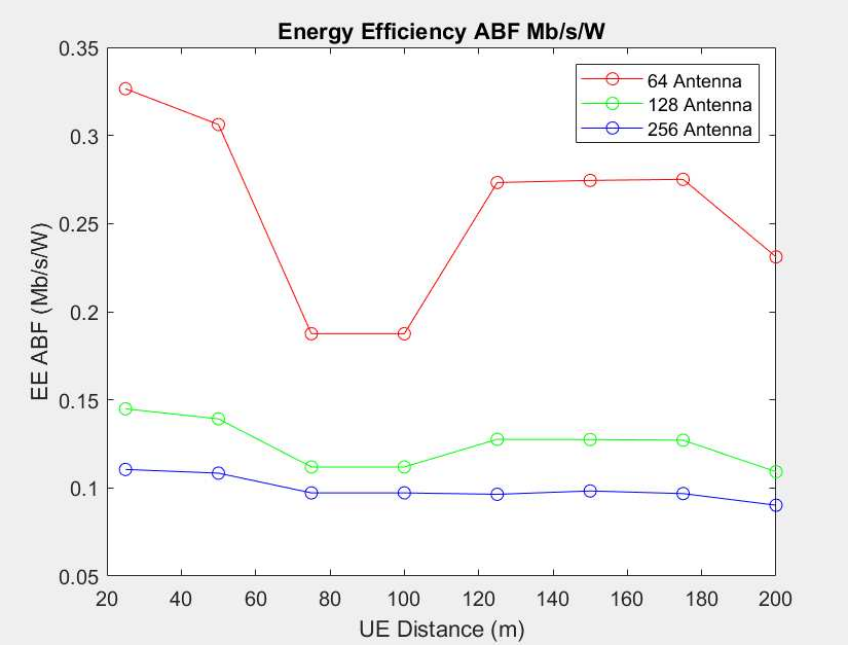

Fig. 11. Energy efficiency of analog beamforming

Figure 11 illustrates the simulation results for the energy efficiency of analog beamforming (ABF) across various antenna configurations. The average energy efficiency values for systems with 64, 128, and 256 antennas are 0.2015, 0.1249, and 0.5552 Mbps/W, respectively. These results indicate a clear trend: the 64-antenna configuration achieves the highest energy efficiency, surpassing both the 128 and 256-antenna setups. Specifically, the 64-antenna configuration exhibits significantly higher energy efficiency compared to the 128-antenna setup, which is, in turn, more efficient than the 256-antenna configuration. This trend may be due to the optimal balance between the number of antennas and the energy consumption associated with each configuration. As the number of antennas increases, power consumption generally rises, which may negate the advantages in energy efficiency, resulting in lower overall performance for the 128 and 256 antenna configurations. These findings underscore the importance of carefully optimizing antenna setups to maximize energy efficiency, especially in situations where power consumption is a critical concern.

Figure 12 presents the simulation results for the energy efficiency (EE) of digital beamforming (DBF) across various antenna configurations. The average EE values for setups with 64, 128, and 256 antennas are 0.5416, 0.5582, and 0.5994 Mbps/W, respectively. Interestingly, the configuration with 256 antennas exhibits the lowest energy efficiency compared to the 128 and 64 antenna setups. Despite having more antennas, the energy efficiency in the 256-antenna configuration is lower. This decline in EE can be attributed to the increased power consumption associated with the 256-antenna setup. While it offers greater spatial diversity and potential capacity, this setup results in diminishing returns in terms of energy efficiency. The higher power consumption in the 256-antenna configuration likely outweighs the advantages gained from the additional antennas, leading to reduced efficiency. In contrast, the 128 and 64-antenna configurations show a more favorable balance between energy consumption and performance, with the 128-antenna setup achieving a slightly higher EE than the 64-antenna configuration. These findings suggest that, in digital beamforming systems, there is an optimal range for the number of antennas that maximizes energy efficiency. Beyond this range, increasing the number of antennas may negatively affect energy performance. This highlights the importance of carefully considering power consumption and antenna configuration when designing energy-efficient beamforming systems.

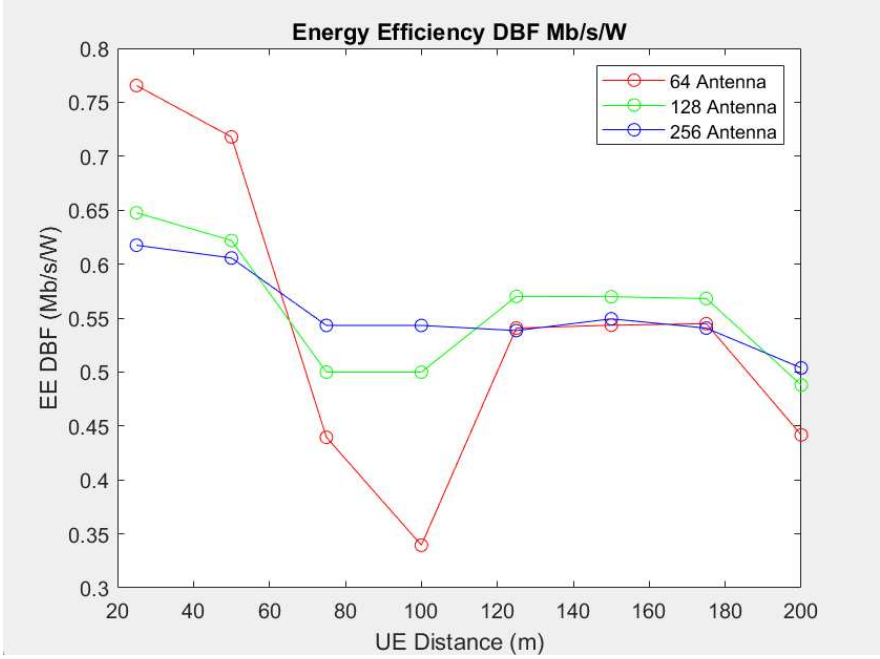

Fig. 12. Energy efficiency of digital beamforming

Figure 13 shows the simulation results for the energy efficiency (EE) of hybrid beamforming (HBF) across different antenna configurations. The average EE values for setups with 64, 128, and 256 antennas are 0.2015, 0.1007, and 0.0835 Mbps/W, respectively. As illustrated in Figure 13, the 64-antenna configuration achieves the highest energy efficiency, while the 256-antenna setup demonstrates the lowest. This notable variation in energy efficiency is mainly due to the increased power consumption associated with the 256-antenna configuration. The higher power demand required to operate the additional antennas leads to a reduction in overall energy efficiency, as power consumption rises more rapidly than performance gains. In contrast, the 64-antenna configuration, despite having fewer elements, strikes a better balance between power consumption and system performance, resulting in higher energy efficiency. The 128-antenna configuration is more efficient than the 256-antenna setup but still requires more power than the 64-antenna configuration, which accounts for its relatively lower energy efficiency.

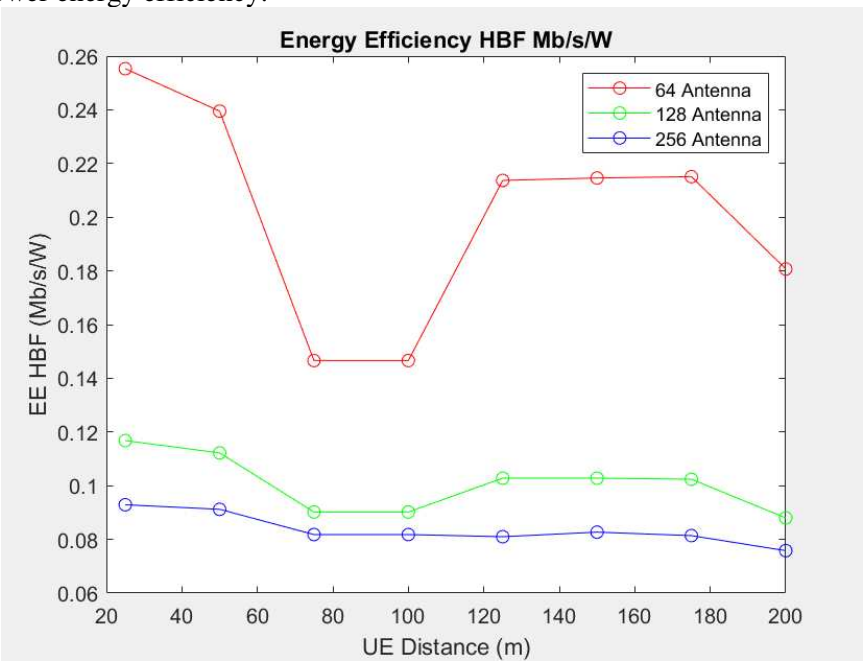

Fig. 13. Energy efficiency of hybrid beamforming

These findings suggest that there is an optimal antenna configuration in hybrid beamforming systems that maximizes energy efficiency. When the number of antennas increases beyond a certain threshold, the additional power consumption may not be justified by performance improvements, leading to diminishing returns in energy efficiency. The results highlight the significance of optimizing antenna configurations to achieve both effective performance and energy savings, especially in systems where energy consumption is a critical factor. Overall, the 64-antenna configuration stands out as the most energy-efficient option, while the 256-antenna configuration is the least efficient due to its higher power requirements.

Table 6 - Average energy efficiency of beamforming methods

Number of Antennas	Beamforming method		
	ABF (Mbps/W)	DBF (Mbps/W)	HBF (Mbps/W)
64	0.2577	0.5416	0.2015
128	0. 1249	0. 5582	0.1007
256	0.5552	0.0994	0.0835

Table 6 presents a comparison of the average energy efficiency for various beamforming methods and antenna configurations. DBF with 128 antennas offers the best balance, achieving the highest EE of 0.5582 Mb/s/W. Compared to hybrid beamforming (HBF) with 256 antennas (0.0835 Mb/s/W), the DBF-128 configuration saves approximately 19% energy in simulated urban macro-cell conditions. These findings align with the trends observed in Borges et al. (2021) and Karimi-Mamaghan et al. (2022), who emphasize optimizing the number of antennas and the beamforming strategy to improve EE in high-frequency environments.

From a practical standpoint, implementing DBF with 128 antennas in real-world 6G deployments is feasible, particularly with ongoing advancements in energy-efficient signal processing hardware. However, the simulations assume ideal power amplifiers; in reality, non-linear power amplifiers may degrade EE, especially at higher output powers, which could narrow the energy gap between DBF and HBF configurations. This hardware consideration should be factored into future experimental studies.

The results also reinforce the validity of applying the Shannon-Hartley theorem in estimating capacity and EE at sub-THz frequencies. As SINR improves, the corresponding data rate scales proportionally, supporting higher throughput per watt. This observation supports findings by Rihan et al. (2020) and Ning et al. (2023), demonstrating that directional beamforming significantly enhances spectrum and energy efficiency.

When contextualized within recent studies, this work provides new insights:

1. While Ning et al. (2023) favor hybrid beamforming for mmWave cost savings, our results suggest DBF is more energy-efficient in sub-THz MU-MIMO under medium-scale antenna configurations.
2. Unlike Siddiqi et al. (2022), which integrates RIS-based beam shaping, this study focuses purely on native beamforming trade-offs, emphasizing that array size optimization alone offers measurable energy gains.

In real-world applications, these findings support the deployment of digital beamforming in urban 6G networks where high EE is required without the complexity and cost of massive arrays. The energy-saving potential of DBF-128 could be beneficial in scenarios with limited infrastructure budgets or where sustainability goals restrict power budgets. In summary, increasing antenna size improves SINR and received power but may reduce energy efficiency due to rising hardware power costs. Digital beamforming with 128 antennas offers the best trade-off, balancing power consumption and spectral performance. These results highlight that optimal performance in 6G systems is not necessarily achieved through maximum scaling, but rather through strategic design of antenna size, beamforming method, and deployment context.

5. Conclusions

This study presented a simulation-based analysis of beamforming performance and energy efficiency in sixth-generation (6G) multi-user MIMO systems operating at sub-terahertz (sub-THz) frequencies. Three beamforming methods—analog, digital, and hybrid—were evaluated across varying antenna configurations (64, 128, and 256 elements). The results show that while increasing antenna array size improves received power and SINR, it also significantly

raises power consumption. Among all configurations, digital beamforming with 128 antennas emerged as the most energy-efficient setup, achieving 0.5582 Mb/s/W, while the 256-antenna hybrid beamforming arrangement showed the poorest energy performance.

These findings offer actionable insights for 6G network design. For urban macro-cell or metro environments, operators should focus on digital beamforming with 128 antennas, which effectively balances signal quality and power usage. Conversely, in rural or low-density scenarios where infrastructure cost and power constraints are more pressing, hybrid beamforming with 64 antennas may provide a more practical solution. These configuration guidelines can help guide the design of energy-aware, scalable 6G base stations.

Despite the strengths of the simulation model, this study is subject to certain limitations. It assumes ideal hardware conditions, including linear power amplifiers, and does not account for real-time hardware impairments. Additionally, the channel model used is primarily LoS-based, which may not fully capture multipath effects in dense environments. Future research should explore joint optimization strategies combining beamforming with intelligent reflecting surfaces (IRS) to further improve energy efficiency and coverage. Moreover, experimental validation with realistic hardware and full-stack protocol considerations will be essential for translating these insights into practical deployment strategies.

Acknowledgment

This work is supported by the professorship research scheme, Universitas Syiah Kuala, under grant no: 125/UN11.2.1/PG.01.03/SPK/PTNBH/2024.

References

Ahmed, A. H., Alrubaee, S. H., Hasan, H. K., & Mohammed, A. H. (2022). Energy efficiency performance for next generation wireless communications. In *2022 International Congress on Human-Computer Interaction, Optimization and Robotic Applications (HORA),* 1–7, IEEE. https://doi.org/10.1109/HORA55278.2022.9800054

Al-Yasir, Y. I. A., Abdulkhaleq, A. M., Parchin, N. O., Elfergani, I. T., Rodriguez, J., Noras, J. M., Abd-Alhameed, R. A., Rayit, A., & Qahwaji, R. (2022). Green and highly efficient MIMO transceiver system for 5G heterogeneous networks. *IEEE Transactions on Green Communications and Networking*, *6*(1), 500–511. https://doi.org/10.1109/TGCN.2021.3100399

Banday, Y., Rather, G. M., & Begh, G. R. (2020). SINR analysis and interference management of macrocell cellular networks in dense urban environments. *Wireless Personal Communications*, *111*, 1645–1665. https://doi.org/10.1007/s11277-019-06947-1

Borges, D., Montezuma, P., Dinis, R., & Beko, M. (2021). Massive MIMO techniques for 5G and beyond—Opportunities and challenges. *Electronics*, *10*(14), 1667. https://doi.org/10.3390/electronics10141667

Dala Pegorara Souto, V., Dester, P. S., Soares Pereira Facina, M., Gomes Silva, D., de Figueiredo, F. A. P., Rodrigues de Lima Tejerina, G., Silveira Santos Filho, J. C., Silveira Ferreira, J., Mendes, L. L., Souza, R. D., & Cardieri, P. (2023). Emerging MIMO technologies for 6G networks. *Sensors*, *23*(4), 1921. https://doi.org/10.3390/s23041921

Damsgaard, H. J., Ometov, A., Mowla, M. M., Flizikowski, A., & Nurmi, J. (2023). Approximate computing in B5G and 6G wireless systems: A survey and future outlook. *Computer Networks*, *233*, 109872. https://doi.org/10.1016/j.comnet.2023.109872

Feng, D., Lai, L., Luo, J., Zhong, Y., Zheng, C., & Ying, K. (2021). Ultra-reliable and low-latency communications: Applications, opportunities and challenges. *Science China Information Sciences*, *64*(12), 120301. https://doi.org/10.1007/s11432-020-2852-1

Hemadeh, I. A., Satyanarayana, K., El-Hajjar, M., & Hanzo, L. (2018). Millimeter-wave communications: Physical channel models, design considerations, antenna constructions, and link-budget. *IEEE Communications Surveys & Tutorials*, *20*(3), 870–913. https://doi.org/10.1109/COMST.2017.2783541

International Telecommunication Union Radiocommunication Sector. (2005). *Recommendation ITU-R P.838-3: Specific attenuation model for rain*. ITU. https://www.itu.int/rec/R-REC-P.838-3-200503-I

Jing, J., Xiaoxue, C., & Yongbin, X. (2016). Energy-efficiency based downlink multi-user hybrid beamforming for millimeter wave massive MIMO system. *Journal of China Universities of Posts and Telecommunications*, *23*(6), 53–62. https://doi.org/10.1016/S1005-8885(16)60045-6

Maccartney, G. R., Rappaport, T. S., Samimi, M. K., & Sun, S. (2015). Millimeter-wave omnidirectional path loss data for small cell 5G channel modeling. *IEEE Access*, *3*, 1573–1580. https://doi.org/10.1109/ACCESS.2015.2465848

Matalatala, M., Deruyck, M., Tanghe, E., Martens, L., & Joseph, W. (2017). Performance evaluation of 5G millimeter-wave cellular access networks using a capacity-based network deployment tool. *Mobile Information Systems*, *2017*, 1–11. https://doi.org/10.1155/2017/3406074

Meena, P., Pal, M. B., Jain, P. K., & Pamula, R. (2022). 6G communication networks: Introduction, vision, challenges, and future directions. *Wireless Personal Communications*, *125*, 1097–1123. https://doi.org/10.1007/s11277-022-09590-5

Muharar, R. Yunida, Y., & Nasaruddin, N. (2024). On the Performance of Multi-Way Massive MIMO Relay With Linear Processing. *IEEE Access*, *12*, 62006-62029. https://doi.org/10.1109/ACCESS.2024.3394596

Nasaruddin, N., Fuady, M., Walidainy, H., & Yunida, Y. (2023). Design and Evaluation of mmWave MIMO Networks Using 28 and 60 GHz in Urban Areas. *Eng. J.*, *27*(11), 73-83. https://doi.org/10.4186/ej.2023.27.11.73

Ning, B., Tian, Z., Mei, W., Chen, Z., Han, C., Li, S., Yuan, J., & Zhang, R. (2023). Beamforming technologies for ultra-massive MIMO in terahertz communications. *IEEE Open Journal of the Communications Society*, *4*, 614–658. https://doi.org/10.1109/OJCOMS.2023.3245669

Rappaport, T. S., Xing, Y., Kanhere, O., Ju, S., Madanayake, A., Mandal, S., Alkhateeb, A., & Trichopoulos, G. C. (2019). Wireless communications and applications above 100 GHz: Opportunities and challenges for 6G and beyond. *IEEE Access*, *7*, 78729–78757. https://doi.org/10.1109/ACCESS.2019.2921522

Rihan, M., Abed Soliman, T., Xu, C., Huang, L., & Dessouky, M. I. (2020). Taxonomy and performance evaluation of hybrid beamforming for 5G and beyond systems. *IEEE Access*, *8*, 74605–74626. https://doi.org/10.1109/ACCESS.2020.2984548

Rinanda, W. E. (2019). Analysis effect of interference on passive repeater microwave link based on ITU-T G821 standard. *Journal of Telecommunication, Electronic and Control Engineering (JTECE)*, *1*(1), 1–10. https://doi.org/10.20895/jtece.v1i01.27

Saeed, A. Yaldiz, H. E., & Alagoz, F. (2023). GHz-to-THz broadband communications for 6G non-terrestrial networks. *ITU Journal on Future and Evolving Technologies*, *4*, 241–250. https://doi.org/10.52953/AOKY1032

Siddiqi, M. Z., & Mir, T. (2022). Reconfigurable intelligent surface-aided wireless communications: An overview. *Intelligent and Converged Networks*, *3*(1), 33-63. https://doi.org/10.23919/ICN.2022.0007

Singh, K., & Katwe, M. (2023). Energy-efficient resource allocation and user grouping for multi-IRS aided MU-MIMO system. *Physical Communication*, *60*, 102147. https://doi.org/10.1016/j.phycom.2023.102147

Walidainy, H., Raihan, S., Adriman, R., Away, Y., & Nasaruddin, N. (2024). Efficiency energy analysis for 6G communication systems using intelligent reflecting surface architecture. *Radioelectronic and Computer Systems*, *2024*(2), 73-84. https://doi.org/10.32620/reks.2024.2.07

Walrand, J., Varaiya, P., 2014. High-Performance Communication Networks Jean Walrand and Pravin Varaiya.

Yu, Y., Ibrahim, R., & Phan-Huy, D.-T. (2022). Dual gradient descent EMF-aware MU-MIMO beamforming in RIS-aided 6G networks. In *2022 20th International Symposium on Modeling and Optimization in Mobile, Ad Hoc, and Wireless Networks (WiOpt)*,383–390, IEEE. https://doi.org/10.23919/WiOpt56218.2022.9930548